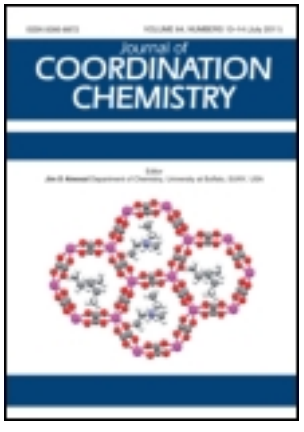

Journal of Coordination Chemistry
Publication details, including instructions for authors and subscription information:
http://www.tandfonline.com/loi/gcoo20

Synthesis and crystal structure of a Schiff base derived from two similar pyrazolone rings and its rare earth complexes: DNA-binding and antioxidant activity

Ming-Fang Wang [a], Zheng-Yin Yang [a], Zeng-Chen Liu [a], Yong Li [a], Tian-Rong Li [a], Mi-Hui Yan [a] & Xiao-Ying Cheng [a]

[a] State Key Laboratory of Applied Organic Chemistry and College of Chemistry and Chemical Engineering, Lanzhou University, Lanzhou 730000, PR China

Accepted author version posted online: 04 Sep 2012.Published online: 17 Sep 2012.

To cite this article: Ming-Fang Wang, Zheng-Yin Yang, Zeng-Chen Liu, Yong Li, Tian-Rong Li, Mi-Hui Yan & Xiao-Ying Cheng (2012) Synthesis and crystal structure of a Schiff base derived from two similar pyrazolone rings and its rare earth complexes: DNA-binding and antioxidant activity, Journal of Coordination Chemistry, 65:21, 3805-3820, DOI: 10.1080/00958972.2012.727208

To link to this article: http://dx.doi.org/10.1080/00958972.2012.727208

Journal of Coordination Chemistry
Vol. 65, No. 21, 10 November 2012, 3805–3820

Synthesis and crystal structure of a Schiff base derived from two similar pyrazolone rings and its rare earth complexes: DNA-binding and antioxidant activity

MING-FANG WANG, ZHENG-YIN YANG*, ZENG-CHEN LIU, YONG LI, TIAN-RONG LI, MI-HUI YAN and XIAO-YING CHENG

State Key Laboratory of Applied Organic Chemistry and College of Chemistry and Chemical Engineering, Lanzhou University, Lanzhou 730000, PR China

(*Received 20 June 2012; in final form 10 August 2012*)

A Schiff base derived from two similar pyrazolone derivatives 4-(1′-phenyl-3′-methyl-5′-hydroxypyrazol-4′-yl)methyleneiminophenazone and its Tb(III) and Dy(III) complexes were synthesized and characterized. The molecular structures of the ligand and Dy(III) complex were determined by X-ray crystal diffraction. The DNA-binding properties of the compounds were investigated by electronic absorption spectroscopy, fluorescence spectra, and viscosity measurements. The compounds interact with DNA through intercalation. The compounds also exhibit potential antioxidant activities *in vitro* and the antioxidant activity of the Ln(III)-complexes was stronger than that of the ligand alone and some standard antioxidants, such as mannitol and vitamin C.

Keywords: 4-(1′-Phenyl-3′-methyl-5′-hydroxypyrazol-4′-yl)methyleneiminophenazone; Spectroscopy; Crystal structure; DNA-Binding mode; Antioxidant activity

1. Introduction

Experiments indicate that the binding study between small molecules and DNA can help design more effective anti-cancer drugs [1, 2] and provide new insights into designing anticancer drugs and developing highly sensitive diagnostic agents [3, 4]. Generally, small molecules bind to DNA in non-covalent modes, such as intercalation, groove-binding, and external electrostatic binding [5, 6]. Applications of metal complexes require that the complexes bind to DNA *via* intercalation, which could induce cellular degradation [7]. Intercalation ability correlates to coordination geometry, ligand donor type, metal ion type and its valence [8, 9]. Lanthanide complexes with tetracycline, phenanthroline, adriamycin, and pyridine have already been synthesized as probes to study nucleic acids [10, 11]; lanthanide ions have much higher coordination numbers and more flexible coordination geometry, which lead to the formation of unusual multidimensional architectures.

*Corresponding author. Email: yangzy@lzu.edu.cn

ISSN 0095-8972 print/ISSN 1029-0389 online © 2012 Taylor & Francis
http://dx.doi.org/10.1080/00958972.2012.727208

Schiff bases and their coordination complexes have attracted attention because of facile syntheses, wide application, and the diverse structural modifications [12–16]. Antipyrine (2,3-dimethyl-1-phenyl-3-pyrazolin-5-one) is the first pyrazolone derivative used in the management of pain and inflammation, and their derivatives have many potential activities including anticancer activity and antimicrobial activity [17, 18]. Schiff bases of 4-aminoantipyrine and their coordination complexes possess applications in biological, clinical, pharmacological, analytical, and materials fields [19].

In this article, the synthesis, characterization, and biological activities of Tb and Dy with 4-(1′-phenyl-3′-methyl-5′-hydroxypyrazol-4′-yl) methyleneiminophenazone Schiff base are presented. The structure of the ligand and Dy(III) complex have been investigated by X-ray crystallography. Some rare earth metal complexes exhibit potential antioxidant activities [20–22]. Since free radicals like hydroxyl are relevant to diseases such as Alzheimers and Parkinsons [23], the *in vitro* antioxidative activities of hydroxyl radical scavenging by metal complexes is of interest.

2. Experimental

2.1. *Materials and instrumentation*

All materials and solvents were of analytical grade and used without purification. 1-Phenyl-3-methyl-5-pyrazole, ethylenediaminetetraaceticacid (EDTA), safranin, 4-aminophenazone, $Dy(NO_3)_3 \cdot 6H_2O$, and $Tb(NO_3)_3 \cdot 6H_2O$ were produced in China. Calf thymus DNA (DNA) and ethidium bromide (EB) were purchased from Sigma Chemical Co. All experiments involved with interaction of the ligand and complexes with DNA were carried out in Tris-HCl buffer (pH = 7.2) containing 5 mmol L^{-1} Tris [Tris(hydroxymethyl)-aminomethane] and 50 mmol L^{-1} NaCl. Solution of DNA gave ratios of absorbance at 260 and 280 nm of about 1.8–1.9 : 1, indicating that the DNA was sufficiently free of protein [24]. DNA concentration per nucleotide was determined by absorption spectroscopy using the molar absorption coefficient ($6600\,(\text{mol}\,L^{-1})^{-1}\,cm^{-1}$) at 260 nm [25]. The ligand and complexes were dissolved in a solvent mixture of 1% methanol and 99% Tris-HCl buffer (pH = 7.2) at 1.0×10^{-5} mol L^{-1}.

Melting point of the ligand was determined on a Beijing XT4-100X microscopic melting point apparatus. IR spectra were obtained in KBr discs on a Therrno Mattson FTIR spectrophotometer from 4000 to 400 cm^{-1}. ^1H NMR spectra were recorded on a Varian VR 400 MHz spectrometer in DMSO-d_6 with TMS as an internal standard. Conductivity measurements were performed in methanol solution with a DDS-11C conductometer at 25°C. UV–Vis spectra were obtained on a Perkin-Elmer Lambda-35 UV–Vis spectrophotometer. Fluorescence measurements were recorded on a Shimadzu RF-5301 spectrofluorophotometer at room temperature. The antioxidant activities were performed in methanol solution with a 721-E spectrophotometer.

2.2. *Preparation of the ligand and its Ln(III) complexes*

Synthesis of L. The synthetic route to L is shown in figure 1. 1-Phenyl-3-methyl-4-formyl-2pyrazolin-5-one (PMFP) was prepared according to the literature [26].

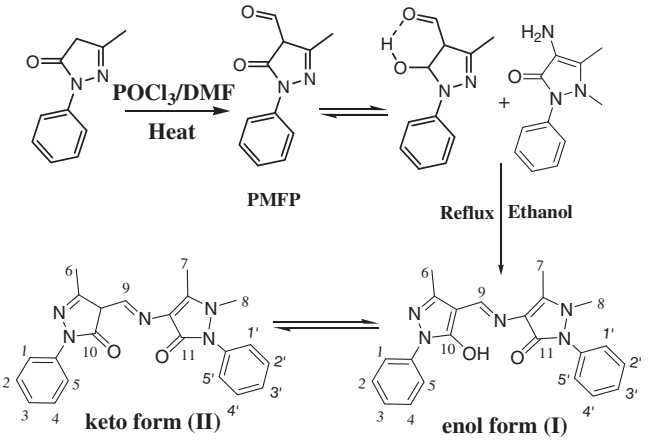

Figure 1. Scheme for synthesis of L.

An ethanol solution (20 mL) of 4-aminophenazone (2.131 g, 10.5 mmol) was added to an ethanol solution (20 mL) of PMFP (2.020 g, 10 mmol). The reaction mixture was refluxed on an oil bath for 8 h with stirring, where upon a yellow precipitate is separated. The precipitate was washed with massive water and ethanol and then recrystallized from ethanol to give the ligand, which was dried under a vacuum. Yield: 2.90 g, 75.15%, m.p.: 222–224°C. IR ν_{max} (cm^{-1}): $\nu(C_{(11)}=O)$ [$\nu(C=O)_{4\text{-aminophenazone}}$]: 1672, $\nu(C=N)$:1632, $\nu(C_{(10)}=O)$ [$\nu(C=O)_{PMFP}$]: 1653. ^1H NMR (400 MHz, DMSO-d_6, ppm): 8.98 (s, 1H, H_9), 7.97 (d, 2H, H_1, $H_{1'}$), 7.48 (t, 2H, H_2, $H_{2'}$), 7.39 (overlap, 5H, H_5, $H_{5'}$, H_4, $H_{4'}$, H_3), 7.15 (t, 1H, $H_{3'}$), 3.11 (s, 3H, $-C_{(6)}H_3$), 2.38 (s, 3H, $-C_{(8)}H_3$), 2.26 (s, 3H, $-C_{(7)}H_3$).

2.3. *Preparation of the complexes*

The ligand (77.4 mg, 0.20 mmol) was dissolved in methanol (20 mL). After 5 min, Tb(III) nitrate (90.6 mg, 0.20 mmol) was added quickly and the solution was refluxed on a water bath for 10 h with stirring. A yellow precipitate, the Tb(III) complex, was separated from the solution by suction filtration, purified by washing several times with methanol and dried for 24 h under vacuum. The Dy(III) complex was prepared in the same way. For the Tb(III) complex: IR ν_{max} (cm^{-1}): $\nu_{(11)C=O}$: 1657, $\nu_{C=N}$: 1594, $\nu_{(10)C=O}$: 1460, ν_{NO3}: 1383, ν_{M-O}: 620, ν_{M-N}: 454 cm^{-1}. U_{max} (nm): 255, 360 nm. Λ_m ($S\,cm^2\,mol^{-1}$): 101 and for Dy(III) complex: IR ν_{max} (cm^{-1}): $\nu_{(11)C=O}$: 1658, $\nu_{C=N}$: 1594, $\nu_{(10)C=O}$: 1456, ν_{NO3}: 1382, ν_{M-O}: 627, ν_{M-N}: 442 cm^{-1}. U_{max} (nm): 257, 350 nm. Λ_m ($S\,cm^2\,mol^{-1}$): 103.

2.4. *Crystal structure determination*

The single crystals of the ligand and Dy(III) complex were obtained in methanol using the diffusing method. A yellow crystal of L ($0.34 \times 0.25 \times 0.20\,mm^3$) was measured on a Bruker Smart-1000 CCD diffractometer with graphite monochromated Mo-Kα radiation ($\lambda = 0.71073$ Å) at 296(2) K. $1.98° < \theta < 25.16°$ for *hkl* ($-9 \le h \le 10$,

$-14 \le k \le 14$, $-22 \le l \le 20$) in the monoclinic system. Yellow crystal of Dy(III) complex ($0.36 \times 0.32 \times 0.27\,mm^3$) was measured on a Bruker Smart-1000 CCD diffractometer with graphite monochromated Mo-Kα radiation ($\lambda = 0.71073$ Å) at 296(2) K. $2.12^\circ < \theta < 28.24^\circ$ for *hkl* ($-20 \le h \le 20$, $-20 \le k \le 30$, $-38 \le l \le 21$) in the orthorhombic system. The positions and anisotropic thermal parameters of all non-hydrogen atoms were refined on F^2 by full-matrix least-squares techniques with the SHELX-97 program package. Absorption corrections were employed using semi-empirical methods from equivalents.

2.5. *DNA binding procedures*

2.5.1. UV absorption measurement. Electronic absorption titration experiments were performed with fixed concentration ($10\,\mu mol\,L^{-1}$), while gradually increasing the concentration of DNA. When measuring the absorption spectra, equal amounts of DNA were added to both the sample and reference solutions to eliminate the absorbance of DNA itself. Each sample solution was scanned from 190 to 500 nm.

2.5.2. Fluorescence spectral titration. Fixed amount ($10\,\mu mol\,L^{-1}$) were titrated with increasing amounts of DNA over a range of DNA concentrations from 2.5 to $30\,\mu mol\,L^{-1}$. The fluorescence spectra from 350 to 600 nm of the above solutions were collected with excitation wavelength of 320 nm. The concentration of the bound compound was calculated using the following equation [27]:

$$C_b = C_t[(F - F_0)/(F_{max} - F_0)],$$

where C_t is the total compound concentration, F is the observed fluorescence emission intensity at given DNA concentration, F_0 is the intensity in the absence of DNA, and F_{max} is the fluorescence of the totally bound compound. Binding data were put into a Scatchard plot of r/C_f *versus* r, where r is the binding ratio $C_b/[DNA]_t$ and C_f is the free compound concentration. All experiments were conducted at room temperature in a Tris-HCl (pH = 7.2) buffer.

2.5.3. Effect of the ligand and complexes on the binding of EB to DNA. Further support for the ligand and complexes binding to DNA *via* intercalation is given through emission quenching experiments. EB is a common fluorescent probe for DNA structure and has been employed in examinations of the mode and process of metal complexes binding to DNA [28]. The solution (2.0 mL) of $5\,\mu mol\,L^{-1}$ DNA and $0.4\,\mu mol\,L^{-1}$ EB (at saturating binding levels) was titrated by 2.5–75 $\mu mol\,L^{-1}$ lanthanide complexes and ligand. The fluorescence spectra from 540 to 700 nm of the solution were collected with excitation wavelength of 525 nm. Quenching data were analyzed according to the Stern–Volmer equation which could be used to determine the fluorescent quenching mechanism:

$$F_0/F = 1 + K_q[Q],$$

where F_0 and F are the fluorescence intensity in the absence and the presence of complex at [Q] concentration, respectively, K_q is the quenching constant, and [Q] is the quencher

concentration. Plots of F_0/F *versus* [Q] appear to be linear and K_q depends on temperature [29].

2.5.4. Effect of ionic strength on the fluorescence spectra. Fluorescence intensities were recorded in the absence and the presence of DNA in solution of each compound and NaCl to investigate salt effects of compounds to DNA.

Iodide quenching experiments were done according to the below methods: fluorescence intensities were recorded in the absence and the presence of DNA in solution of each compound and KI. The fluorescence quenching efficiency is evaluated by Stern–Volmer K_{sv}, which varies with the experimental conditions. Quenching plots were constructed according to the following Stern–Volmer equation:

$$F_0/F = 1 + K_{sv}[I^-],$$

where F_0 and F are the fluorescence intensity in the absence and the presence of iodide at $[I^-]$ concentration, respectively, K_{sv} is the quenching constant, and $[I^-]$ is the concentration of iodide. Plots of F_0/F *versus* $[I^-]$ appear to be linear and K_{sv} was evaluated by linear least-squares analysis of the data [30].

2.5.5. Viscosity measurements. Viscosity experiments were conducted on an Ubbelodhe viscometer immersed in a thermostated water bath maintained at 25.0 ± 0.1°C. Titrations were performed for the ligand and complexes (0.5–4 μmol L^{-1}), and each compound was introduced into a DNA solution (5 μmol L^{-1}) present in the viscometer. Data were analyzed as $(\eta/\eta_0)^{1/3}$ *versus* the ratio of the concentration of the compound and DNA, where η is the viscosity of DNA in the presence of the compound and η_0 is the viscosity of DNA alone [31, 32]. Viscosities were calculated from the observed flow time of solutions containing DNA corrected for the flow time of buffer alone (t_0), $\eta = t - t_0$.

2.6. *Scavenger measurements of hydroxyl radical (OH•)*

Hydroxyl radicals (OH•) in aqueous media were generated through the Fenton reaction [33]. Solutions of the test compounds were prepared with DMF. The reaction mixture contained 2.0 mL of 0.15 mol L^{-1} phosphate buffer (pH = 7.4), 1.0 mL of 114 μmol L^{-1} safranin, 1 mL of 945 μmol L^{-1} EDTA–Fe(II), 1 mL of 3% H_2O_2 and 30 μL of the test compound solution (the final concentration: $C_{i(i=1-6)} = 1.0$, 2.0, 3.0, 4.0, 5.0, 6.0 μmol L^{-1}). Sample without the test compound was used as the control. Reaction mixtures were incubated at 37°C for 60 min in a water bath. Absorbances (A_i, A_0, A_c) at 520 nm were measured. The scavenging ratio is defined as

$$\text{Suppression ratio } (\%) = [(A_i - A_0)/(A_c - A_0)] \times 100\%,$$

where A_i = absorbance in the presence of the test compound; A_0 = absorbance of the blank in the absence of the test compound; A_c = absorbance in the absence of the test compound, EDTA–Fe(II) and H_2O_2. The antioxidant activity was expressed as the 50% inhibitory concentration (IC_{50}). IC_{50} values were calculated from regression lines where x was the test compound concentration in μmol L^{-1} and y was percent inhibition of the test compounds.

3. Results and discussion

3.1. *Characterization and structures of the complexes*

The ligand and its complexes are stable in atmospheric conditions for extended periods and easily soluble in DMF and DMSO; slightly soluble in ethanol, methanol, and acetone; insoluble in benzene, water, and diethyl ether. Crystals of the ligand and Dy(III) complex were obtained from methanol and diethyl ether diffusing method. The molar conductivities of the complexes are $102\,S\,cm^2\,mol^{-1}$ in methanol solution and in accord with them being formulated as 1 : 1 electrolytes [34].

The IR bands of the ligand at 1672, 1653, and $1632\,cm^{-1}$ are ν(C=O) of the 4-aminoantipyrine, ν(C=O) of the PMFP and ν(C=N), respectively. Thus the ligand exists in the keto form in the solid state. However, in spectra of the complexes, these are replaced by bands at 1657, 1594, and $1458\,cm^{-1}$, respectively, and a new band is observed at $1458\,cm^{-1}$ due to ν(C–O$^-$). It is concluded that the ligand reacts in the enol form (I) when coordinated to the metal. Weak bands at 448 and $628\,cm^{-1}$ are allocated as ν(M–N) and ν(M–O). The shifts and new bands further confirmed that nitrogen of imino and oxygen of carbonyl coordinated with the metal [35, 36]. Additionally, an intense band associated with the asymmetric stretch of nitrate is observed at $1384\,cm^{-1}$, establishing that the complexes contain free nitrate (C_{2v}).

3.2. *Description of the crystal structure*

The crystallographic data for the ligand and Dy(III) complex are given in table 1 and selected bond lengths and angles are listed in tables 2 and 3, respectively. The ligand crystallizes in the monoclinic lattice with a space group of $P2_1/n$. Each unit cell contains four molecules. The distances for $C_{(11)}$–O, $C_{(11)}$–C, $C_{(10)}$–O, and $C_{(10)}$–C are 1.229(2), 1.430(2), 1.250(2), and 1.429(2) Å, respectively, so the ligand is in the keto form (II) in figure 1. An ORTEP representation of the ligand and Dy(III) complex are shown in figure 2. The Dy(III) complex crystallizes into an orthorhombic lattice with the space group *Pbca*. The complex is mononuclear and coordination of ligand to Dy(III) results in formation of two five-membered (DyOCCN) and six-membered (DyNCCCO) chelate rings. The Dy(III) is coordinated by two ONO tridentate ligands with two nitrogen atoms of azomethine nitrogen (N4, N7), two PMFP-pyrazolone oxygen atoms (O39, O91), and another two 4-antipyrine pyrazolone oxygen atoms (O3, O12). There are also coordinated water O1 and methanol O5. The distances in the Dy(III) complex for $C_{(10)}$–O, $C_{(10)}$–C are 1.253(9), 1.401(9), 1.272(9), and 1.403(11) Å. Compared to the ligand, the $C_{(10)}$–O distance lengthened and the $C_{(10)}$–C distance is shorter. The distances in the Dy(III) complex for $C_{(10)}$–O are between C–O (1.41–1.44 Å) and C=O (1.19–1.23 Å) [37], suggesting that the oxygen of pyrazole ring take part in coordination in the enolic form. Distances for $C_{(10)}$–C are between C–C (1.47–1.53 Å) and C=C (1.32–1.38 Å), supporting this conclusion. In the complex, the ligand in the enol form (I) loses one proton and is a tridentate chelating agent. The analytical results indicate that the Dy(III) complex has 1 : 2 metal to ligand stoichiometry by coordination at the Dy(III) center. However, in papers reported in our group, the general formulas of complexes were $Ln(HL)_3$, with tricapped trigonal prism coordination polyhedra. The difference might be because geometric constraints were applied to these molecules to ensure stable refinement.

Table 1. Crystal data and experimental data of the ligand and Dy(III) complex.

Compound	L	$[DyL_2(CH_3OH)(H_2O)]\cdot[NO_3(CH_3OH)_2]$
Empirical formula	$C_{22}H_{21}N_5O_2$	$C_{47}H_{46}DyN_{11}O_{11}$
Formula weight	387.44	1103.50
Crystal color	Yellow	Yellow
Crystal size (mm^3)	$0.34\times0.25\times0.20$	$0.36\times0.32\times0.27$
Temperature (K)	296(2)	296(2)
Wavelength (Å)	0.71073	0.71073
Radiation	Mo-Kα	Mo-Kα
Crystal system	Monoclinic	Orthorhombic
Space group	$P2_1/n$	$Pbca$
Z	4	8
Unit cell dimensions (Å, °)		
a	8.4100(3)	15.7620(13)
b	12.3782(4)	22.5619(18)
c	18.7118(6)	28.864(2)
α	90.00	90.00
β	95.204(2)	90.00
γ	90.00	90.00
Volume ($Å^3$)	1939.88(11)	10264.7(15)
Calculated density ($g\,cm^{-3}$)	1.327	1.428
Absorption coefficient (mm^{-1})	0.088	1.523
$F(000)$	816	4472
θ range for data collection (°)	1.98–25.16	1.72–28.24
Index ranges	$-9\le h\le10$	$-20\le h\le20$
	$-14\le k\le14$	$-20\le k\le29$
	$-22\le l\le20$	$-38\le l\le21$
Reflections collected	3461	12,255
Independent reflections	2228 (R(int) = 0.0427)	6245 (R(int) = 0.0584)
Refinement method	Full matrix least-squares on F^2	Full matrix least-squares on F^2
Data/restraints/parameters	3461/0/269	12,255/0/631
Goodness-of-fit on F^2	1.014	0.982
Final R indices [$I>2\sigma(I)$]	$R_1=0.0427$, $wR_2=0.0943$	$R_1=0.0584$, $wR_2=0.1531$
R indices (all data)	$R_1=0.0792$, $wR_2=0.1108$	$R_1=0.1372$, $wR_2=0.1892$

Table 2. Selected bond lengths (Å) for the ligand.

Bond names	Bond lengths
O1–C12	1.229(2)
C12–C13	1.430(2)
C10–C13	1.350(2)
O2–C17	1.250(2)
C16–C17	1.429(2)
N1–C30	1.320(2)

All these results suggest that the formula of the complexes is $[ML_2(CH_3OH)(H_2O)]\cdot[NO_3(CH_3OH)_2]$.

3.3. *DNA-binding studies*

3.3.1. UV absorption measurement. Electronic absorption spectra of the ligand and its lanthanide complexes in the absence and the presence of DNA (at a constant

Table 3. Selected bond lengths (Å) and angles (°) for Dy(III) complex.

Bond names	Bond lengths	Bond names	Bond angles
Dy1–O5	2.251(5)	O5–Dy1–O39	90.8(2)
Dy1–O39	2.270(5)	O5–Dy1–O3	144.58(18)
Dy1–O3	2.384(5)	O39–Dy1–O3	76.81(19)
Dy1–O1	2.388(5)	O5–Dy1–O1	144.90(19)
Dy1–O91	2.393(6)	O39–Dy1–O1	105.09(18)
Dy1–O12	2.395(5)	O3–Dy1–O1	70.40(17)
Dy1–O10	2.425(4)	O5–Dy1–O91	93.4(2)
Dy1–N4	2.560(6)	O39–Dy1–O91	79.1(2)
Dy1–N7	2.581(6)	O3–Dy1–O91	91.7(2)
C10–O39	1.253(9)	O1–Dy1–O91	74.63(19)
C10–C20	1.401(11)	O5–Dy1–N7	75.50(19)
C9–O12	1.249(9)	O39–Dy1–N7	73.83(19)
C9–C54	1.409(10)	O3–Dy1–N7	69.21(18)
C22–O5	1.272(9)	O1–Dy1–N7	138.66(18)
C22–C92	1.403(11)	O91–Dy1–N7	72.5(2)
C67–O3	1.260(8)	O5–Dy1–N7	131.97(18)
C67–C72	1.434(10)	N4–Dy1–N7	137.55(19)

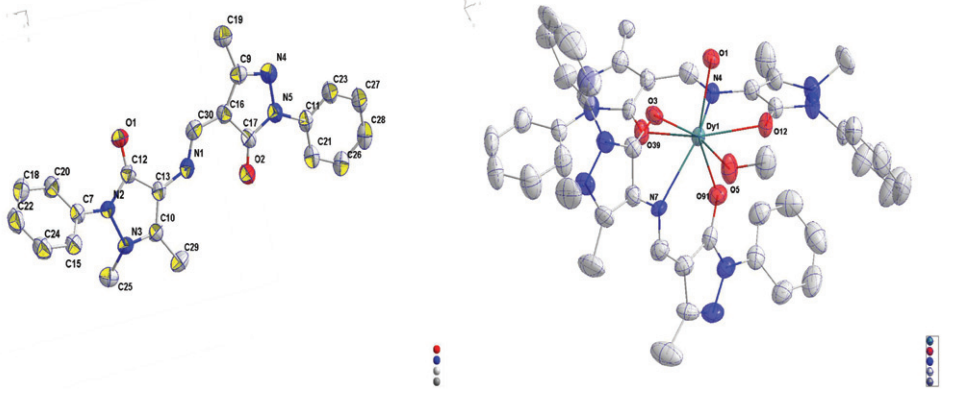

Figure 2. ORTEP view of the ligand (left) and Dy(III) complex (right) showing atom numbering and 30% probability thermal ellipsoids for non-hydrogen atoms.

concentration of the compounds) are shown in figure 3. With increasing DNA concentrations the absorption bands at about 255 nm and 365 nm of the compounds show hypochromism and a red shift of 5 nm. These spectral characteristics indicate strong stacking interaction between an aromatic chromophore and base pairs of DNA, suggesting that the compounds might bind to DNA by intercalation [38]. After intercalating the base pairs of DNA, the π^* orbital of the intercalated ligand could couple with a π orbital of base pairs, thus decreasing the π–π^* transition energy, and further resulting in the bathochromism. The coupling π^* orbital was partially filled by electrons, decreasing the transition probabilities, and concomitantly resulting in hypochromism [39].

In order to further test if the compounds could bind to DNA by intercalation, EB (a typical indicator of intercalation) is employed [40]. Figure 4 shows that the maximal

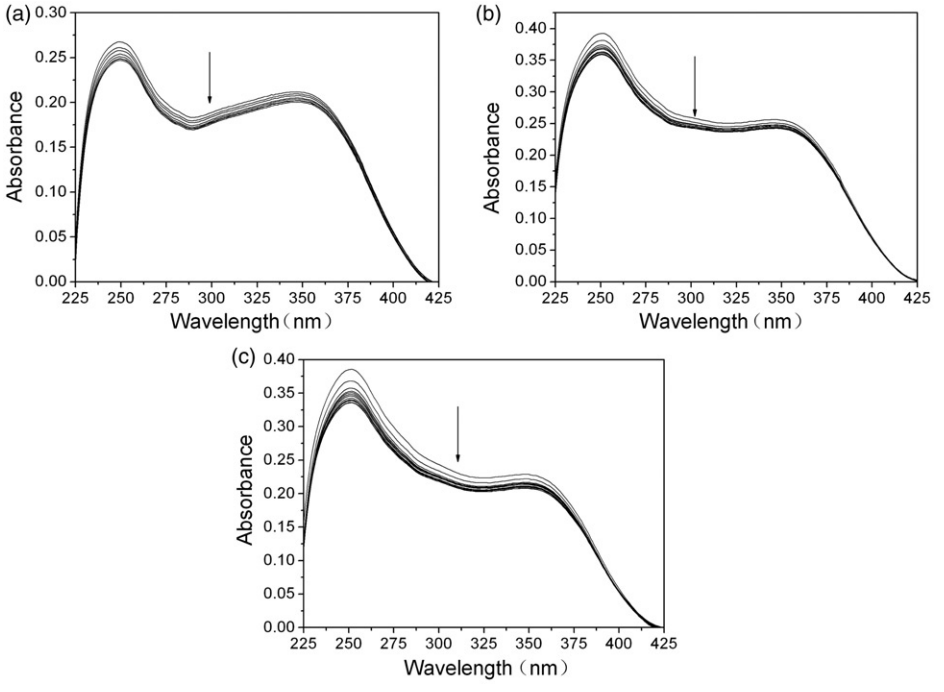

Figure 3. Electronic absorption spectral change of the free ligand (a), Tb(III) (b), Dy(III) (c) complexes ($10\,\mu mol\,L^{-1}$) in the absence and the presence of increasing amounts of ct-DNA (2.5, 5.0, 7.5, 10.0, 12.5, 15.0, 17.5, and $20.0\,\mu mol\,L^{-1}$). Arrows show the absorbance changes upon increasing DNA concentration.

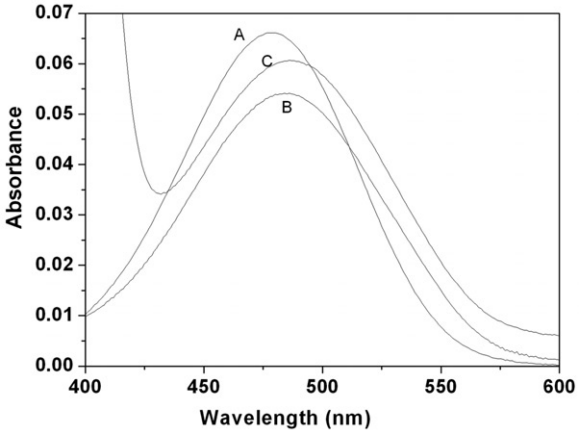

Figure 4. Visible absorption spectra of $1 \times 10^{-5}\,mol\,L^{-1}$ EB (curve A); (A) + $2.5 \times 10^{-5}\,mol\,L^{-1}$ DNA (curve B); (B) + $2.5 \times 10^{-5}\,mol\,L^{-1}$ Dy(III) complex (curve C) in Tris-HCl buffer ($5\,mmol\,L^{-1}$ Tris-HCl, $50\,mmol\,L^{-1}$ NaCl, pH = 7.20) solution.

absorption of EB at 475 nm (curve A) decreased and shifted to 480 nm (curve B) in the presence of DNA, which is the characteristic of intercalation. Curve C is the absorption of a mixture solution of EB, DNA, and the Dy(III) complex. The absorption at 488 nm increased compared with curve B. This could result from two reasons: (1) there may

exist competitive intercalation between Dy(III) complex and EB with DNA, releasing some free EB from the DNA–EB system and (2) EB binds to Dy(III) complex strongly, resulting in a decreased amount of EB intercalated into DNA. However, no new absorption peaks were observed, so the second reason could be ruled out.

3.3.2. Fluorescence spectra titration. The steady-state emission spectra of 10 μmol L^{-1} solutions of the free ligand and its lanthanide complexes in Tris-HCl buffer show an increase in the emission intensity with successive addition of DNA at room temperature (figure 5). According to the Scatchard equation, a plot of r/C_f *versus* r gave K_b values of $(2.44 \pm 0.24) \times 10^5$, $(3.63 \pm 0.26) \times 10^5$, and $(5.32 \pm 0.76) \times 10^5$ $(\text{mol L}^{-1})^{-1}$ from the fluorescence data for the ligand, Tb(III), and Dy(III) complexes, respectively. In the same calculation method and experimental conditions, the K_b values of two rare earth complexes were compared with other known DNA-intercalative complexes, like $[EuL \cdot (NO_3)_2] \cdot NO_3$, 2.48×10^5 $(\text{mol L}^{-1})^{-1}$ [41], $[LaL_2 \cdot (NO_3)_2] \cdot NO_3$, $(2.2 \pm 0.3) \times 10^5$ $(\text{mol L}^{-1})^{-1}$, $[SmL_2 \cdot (NO_3)_2] \cdot NO_3$, $(4.0 \pm 0.6) \times 10^5$ $(\text{mol L}^{-1})^{-1}$, $[NdL_2 \cdot (NO_3)_2] \cdot NO_3$, $(7.6 \pm 0.9) \times 10^5$ $(\text{mol L}^{-1})^{-1}$, and $[YbL_2 \cdot (NO_3)_2] \cdot NO_3$, $(3.1 \pm 0.5) \times 10^5$ $(\text{mol L}^{-1})^{-1}$ [42]. The K_b values have no notable difference between the two rare earth complexes and the above known DNA-intercalative complexes. The three compounds have good ability to bind to DNA. Results obtained from the

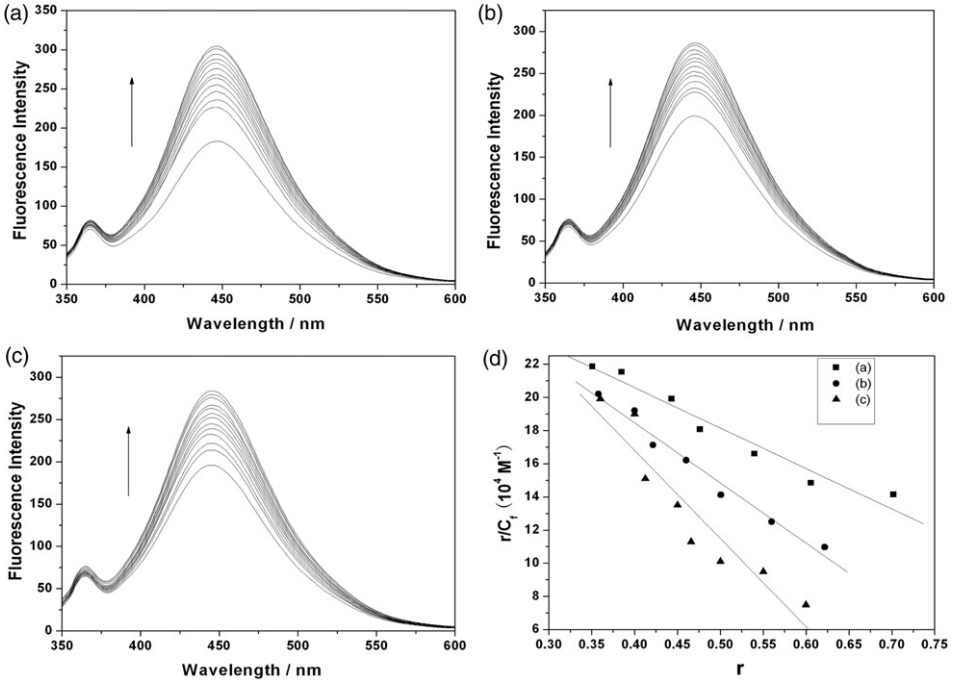

Figure 5. Emission enhancement spectra of free ligand (a), Tb(III) (b) and Dy(III) (c) complexes (10 μmol L^{-1}) in the presence of 0, 2.5, 5.0, 7.5, 10.0, 12.5, 15.0, 17.5, 20, 22.5, 25, 27.5, and 30.0 μmol L^{-1} DNA. Arrows show the emission intensity changes upon increasing DNA concentration. Scatchard plot of the fluorescence titration data of ligand and metal complexes (d), K_b (a): $(2.44 \pm 0.24) \times 10^5$, K_b (b): $(3.63 \pm 0.26) \times 10^5$, K_b (c): $(5.32 \pm 0.76) \times 10^5$ $(\text{mol L}^{-1})^{-1}$.

fluorescence spectra suggest that all the compounds are protected from water by the hydrophobic environment inside the DNA helix and that the metal complexes can be protected more efficiently than the ligand alone. Since the hydrophobic environment inside the DNA helix reduces the accessibility of solvent water to the compound and the compound mobility is restricted at the binding site, a decrease of the vibrational modes of relaxation results. The binding affinities of the complexes are attributed to the extension of the π system of the intercalated ligand and the coordination of rare earth ion. However, the DNA binding modes and binding affinity need to be proved further by viscosity studies and EB-DNA competitive experiment.

3.3.3. Effect of the ligand and complexes on the binding of EB to DNA. It is well known that EB is one of the most sensitive fluorescence probes that can intercalate nonspecifically into DNA effectively increasing the fluorescence of EB [43]. Competitive binding to DNA of the compounds with EB provides indirect evidence for DNA binding mode. The emission spectra of EB bound to DNA in the absence and the presence of each compound have been recorded for $[EB] = 4 \times 10^{-7}\,mol\,L^{-1}$, $[DNA] = 5 \times 10^{-6}\,mol\,L^{-1}$ with increasing amounts for each compound (figure 6). The K_q values for the ligand, Tb(III) and Dy(III) complexes are $(0.96 \pm 0.01) \times 10^4$,

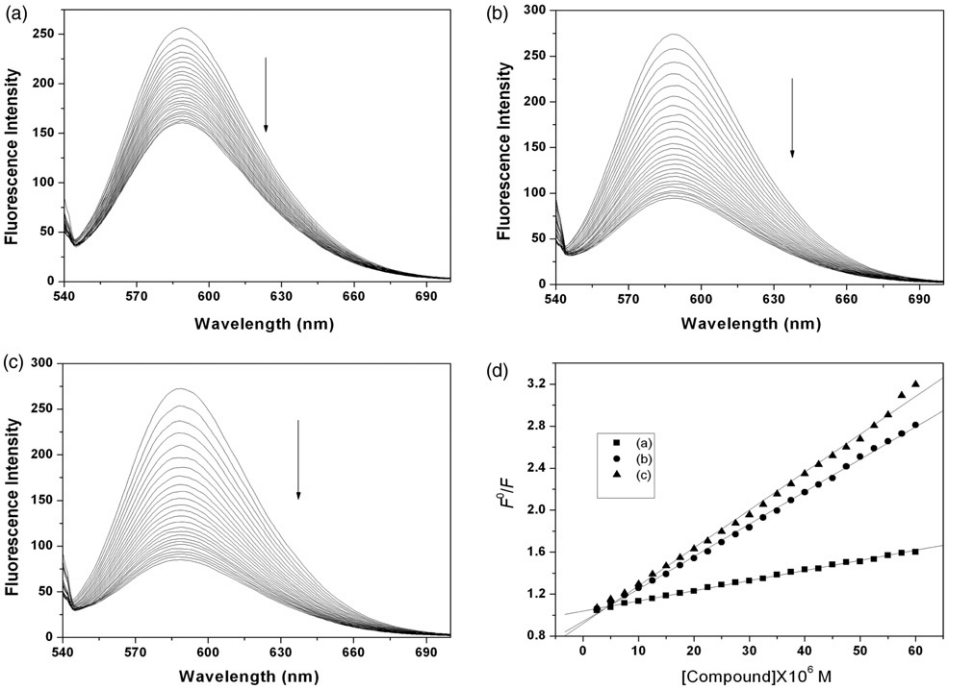

Figure 6. Emission spectra of DNA-EB system $\lambda_{ex} = 525\,nm$, $\lambda_{em} = 540$–$700\,nm$, in the presence of the ligand (a), Tb(III) (b) and Dy(III) complexes (c) (0, 2.5, 5, 7.5, 10, 12.5, 15, 17.5, 20, 22.5, 25, 27.5, 30, 32.5, 35, 37.5, 40, 42.5, 45, 47.5, 50, 52.5, 55, 57.5, and $60\,\mu mol\,L^{-1}$). Arrows show the emission intensity changes upon increasing the ligand and the complexes. Stern-Volmer plot of the fluorescence titration data of ligand and complexes (d), K_q (a): $(0.96 \pm 0.01) \times 10^4$, K_q (b): $(3.09 \pm 0.02) \times 10^4$, K_q (c): $(3.61 \pm 0.05) \times 10^4$ $(mol\,L^{-1})^{-1}$.

$(3.09 \pm 0.02) \times 10^4$, and $(3.61 \pm 0.05) \times 10^4 \,\mathrm{mol\,L^{-1}}$, respectively. The quenching plots illustrate that quenching of EB bound to DNA by the compounds is in agreement with the linear Stern–Volmer equation and the binding ability follows the order Dy(III) complex > Tb(III) complex > L, which is in agreement with the fluorescence titration and viscosity measurements.

3.3.4. Effect of ionic strength on the fluorescence spectra. DNA is an anionic polyelectrolyte with phosphate groups. Monitoring the spectral change with different ionic strength is an efficient method for distinguishing the binding modes between metal complex and DNA. NaCl is used to control the ionic strength of the solutions. The addition of Na^+ can neutralize the negatively charged phosphate groups, so Na^+ would weaken the electrostatic interaction between DNA and molecules [44]. If the compound binds to DNA through an electrostatic interaction mode, the surface of DNA will be surrounded by the sodium ions with the increasing ionic strength. Then the compound is difficult to approach DNA molecules and the strength of interaction with DNA decreases, and then the degree of fluorescence quenching also decreases [45, 46]. As seen from figure 7, addition of NaCl to the Dy (III) complex in the presence of DNA has a little increase on the fluorescence intensity, showing that the interaction of the Dy(III) complex with DNA is not an electrostatic interaction.

Iodide and ferrocyanide anions quench fluorescence of complexes very efficiently in aqueous solution; we used potassium iodide as the quencher to determine the relative accessibilities of free and bound Dy(III) complex. Emission spectra for Dy(III) complex and potassium iodide with the absence of DNA are illustrated in the titration curves (figure 8a). Compared to Dy(III) complex alone, emission intensity decreases with increasing concentrations of potassium iodide regardless of the buffer solution containing DNA. The quenching plots illustrate that the quenching studies of the Dy(III) complex are in good agreement with the linear Stern–Volmer equation and the slopes were calculated by the linear least-squares method. The observed quenching constants (K_{sv}) were 7.42 and 12.68 $(\mathrm{mol\,L^{-1}})^{-1}$ with and without DNA, respectively.

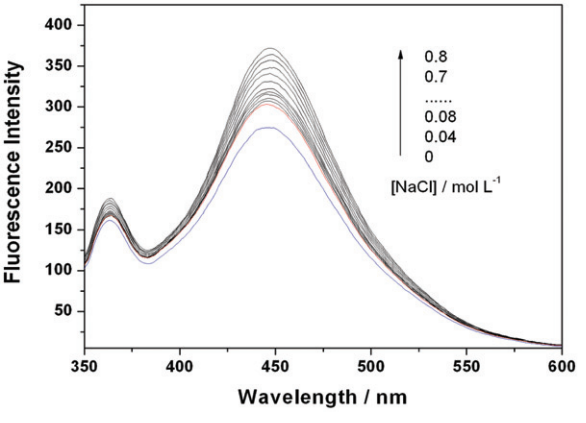

Figure 7. Fluorescence spectra of Dy(III) complex ($10\,\mu\mathrm{mol\,L^{-1}}$)-DNA ($10\,\mu\mathrm{mol\,L^{-1}}$) in different concentrations of NaCl (0, 0.04, 0.08, 0.12, 0.16, 0.20, 0.3, 0.4, 0.5, 0.6, 0.7, and $0.8\,\mathrm{mol\,L^{-1}}$). Arrow shows the increase of NaCl concentrations.

When the complex was bound to the DNA helix, the K_{sv} was smaller. Similar results can be obtained for the ligand and Tb(III) complex and we conclude that the compounds interact with the DNA helix and they are protected from the anionic quencher, owing to the base pairs above and below the compounds [47].

3.3.5. Viscosity measurements. Hydrodynamic measurements (i.e., viscosity and sedimentation), which are sensitive to DNA length changes, are regarded as the least ambiguous and most critical test of binding in solution in the absence of crystallographic structural data [48]. A classical intercalation model demands that the DNA helix lengthens as base pairs are separated to accommodate the bound ligand, leading to an increase of DNA viscosity. In contrast, partial, non-classical intercalation of ligand could bend (or kink) the DNA helix reducing its effective length and, concomitantly, its viscosity [49]. Hence, viscosity study is applied to clarify the binding of these compounds with DNA. Figure 9 shows that the compounds cause significant increase in the viscosity of DNA. Viscosity measurement clearly shows that the compounds can

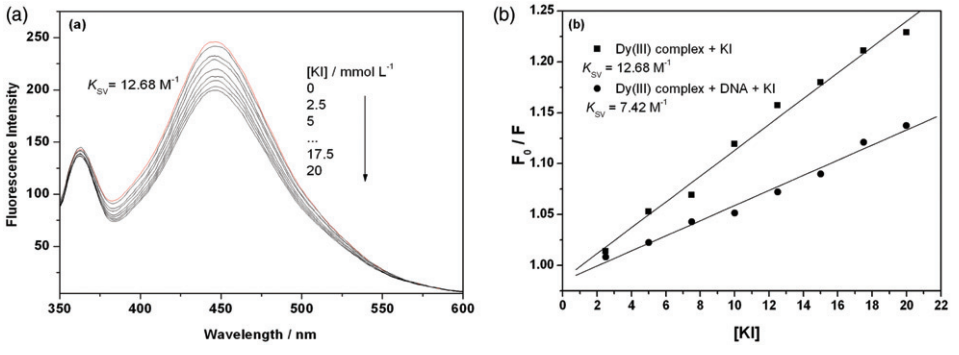

Figure 8. (a) Fluorescence spectra of Dy(III) complex (10 μmol L^{-1}) with increasing concentration of KI (0, 2.5, 5, 7.5, 10, 12.5, 15, 17.5, and 20 mmol L^{-1}). (b) Stern–Volmer plot of the fluorescence titration data of Dy(III) complex. Effect of KI concentration (1: Dy(III) complex + KI; 2: Dy(III) complex + KI + DNA). K_{sv} (1) = 12.68 (mol L^{-1})$^{-1}$, K_{sv} (2) = 7.42 (mol L^{-1})$^{-1}$.

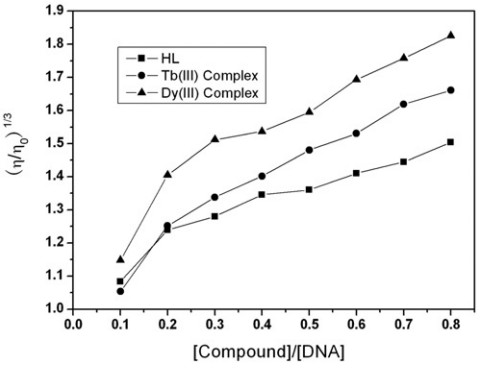

Figure 9. Effects of increasing amounts of the ligand, Tb(III) and Dy(III) complexes on the relative viscosity of DNA at 25.0 ± 0.1°C.

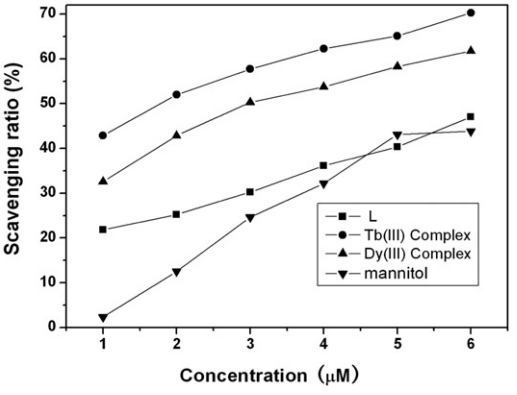

Figure 10. Scavenging effects of the ligand, Tb(III), and Dy(III) complexes and manitol on hydroxyl radical.

intercalate between adjacent DNA base pairs, causing an extension in the helix and thus increase the viscosity of DNA, and that the complexes can intercalate stronger than the free ligand.

On the basis of all the spectroscopic studies and the viscosity measurement, the ligand, Tb(III) and Dy(III) complexes proved that they can bind to DNA in an intercalative mode and the Dy(III) complex exhibits strongest binding affinity to DNA.

3.4. *Scavenger measurements of OH·*

Since the synthesized ligand and its lanthanide complexes exhibit good DNA binding affinity, we investigate their antioxidant activity. Reactive oxygen species (ROS), such as superoxide anion and hydroxyl radical, are usually generated by all aerobic cells during normal oxygen metabolism, and the oxidation induced by ROS is involved in the pathogenesis of various diseases through direct effects on DNA and by acting as a tumor promoter [50]. Consequently, the antioxidant activity of the ligand and its lanthanide complexes is studied by comparing their scavenging effects on hydroxyl radical ($OH^{\bullet}$) in KH_2PO_4–Na_2HPO_4 buffer solution.

The inhibitory effect of the compounds is marked and the average suppression ratio for $OH^{\bullet}$ increases with increasing compound concentration (figure 10). The values of IC_{50} of the ligand, Tb(III), Dy(III) complexes and mannitol for hydroxyl radical scavenging effects are 10.12, 1.699, 3.012, and 10.19 μmol L^{-1}, respectively (table 4), which indicates that formation of metal-ligand coordination complex enhances the scavenger effect.

4. Conclusion

A Schiff base 4-(1′-phenyl-3′-methyl-5′-hydroxypyrazol-4′-yl) methyleneiminophenazone and its Ln(III) complexes have been prepared and characterized. Structures of the ligand and Dy(III) complex were determined by X-ray single-crystal diffraction.

Table 4. Scavenging effects of the ligand, Tb(III), and Dy(III) complexes and mannitol on OH·.

Compound	Average inhibition (%) for OH· (μmol L^{-1})						Equation	IC_{50} (μmol L^{-1})	R^2
	1.0	2.0	3.0	4.0	5.0	6.0			
HL	21.85	25.21	30.25	36.13	40.34	47.06	$y = 31.26x + 18.58$	10.12	0.946
Tb(III) complex	42.86	52.00	57.71	62.29	65.14	70.28	$y = 34.06x + 42.16$	1.699	0.995
Dy(III) complex	32.57	42.86	50.28	53.71	58.29	61.71	$y = 37.19x + 32.19$	3.012	0.998
Mannitol	2.30	12.52	24.63	32.19	43.09	43.83	$y = 57.26x - 0.73$	10.19	0.958

DNA binding properties and antioxidant activities were studied systematically. Results indicate that the ligand and its complexes bind to DNA *via* intercalation and the complexes have better DNA binding affinity than the free ligand. Furthermore, the complexes have more active scavenging effects on OH·. Our work clearly indicates that rare earth-based complexes have practical applications, such as understanding the mechanisms of interaction between small molecules and DNA, the development of potential anticancer drugs and new antioxidants.

Supplementary material

Crystallographic data for the structural analysis have been deposited with the Cambridge Crystallographic Data Centre, CCDC (842956). Copy of this information may be obtained free of charge from the Director, CCDC, 12 Union Road, Cambridge, CB2 1EZ, UK (Fax: +44-1223-336033; E-mail: deposit@ccdc.cam.ac.uk or http://www.ccdc.cam.ac.uk/deposit).

Acknowledgments

This work is supported by the National Natural Science Foundation of China (20975046, 81 171 337).

References

[1] K.E. Erkkila, D.T. Odom, J.K. Barton. *Chem. Rev.*, **99**, 2777 (1999).
[2] H. Mansouri-Torshizi, M. I-Moghaddam, A. Divsalar, A.A. Saboury. *Bioorg. Med. Chem.*, **16**, 9616 (2008).
[3] R. Blasius, C. Moucheron, A.K. Mesmaeker. *Eur. J. Inorg. Chem.*, 3971 (2004).
[4] G.W. Zhang, J.B. Guo, J.H. Pan, X.X. Chen, J.J. Wang. *J. Mol. Struct.*, **923**, 114 (2009).
[5] D. Karlin. *Progress in Inorganic Chemistry Kenneth*, Vol. 57, John Wiley & Sons, Inc., Hoboken, NJ (2011).
[6] R. Palchaudhuri, P.J. Hergenrother. *Curr. Opin. Biotech.*, **18**, 497 (2007).
[7] N. Raman, A. Selvan. *J. Coord. Chem.*, **64**, 534 (2011).
[8] H. Zhang, C.S. Liu, X.H. Bu, M. Yang. *J. Inorg. Biochem.*, **99**, 1119 (2005).
[9] M. Asadi, E. Safaei, B. Ranjbar, L. Hasani. *New J. Chem.*, **28**, 1227 (2004).
[10] Y.X. Ci, Y.Z. Li, W.B. Chang. *Anal. Chim. Acta*, **248**, 589 (1991).

[11] M. Elbanowski, B. Makowska. *J. Photochem. Photobiol. A Chem.*, **99**, 85 (1996).
[12] G.C. Xu, L. Zhang, L. Liu, G.F. Liu, D.Z. Jia. *Polyhedron*, **27**, 12 (2008).
[13] S. Kotha. *Acc. Chem. Res.*, **36**, 342 (2003).
[14] H.C. Wu, P. Thanasekaran, C.H. Tsai, J.Y. Wu, S.M. Huang, Y.S. Wen, K.L. Lu. *Inorg. Chem.*, **45**, 295 (2005).
[15] J.L. Sessler, E. Tomat, V.M. Lynch. *J. Am. Chem. Soc.*, **128**, 4184 (2006).
[16] S. Das, A. Nag, D. Goswami, P.K. Bharadwaj. *J. Am. Chem. Soc.*, **128**, 402 (2006).
[17] S. Bondock, R. Rabie, H.A. Etman, A.A. Fadda. *Eur. J. Med. Chem.*, **43**, 2122 (2008).
[18] N. Raman, A. Selvan. *J. Mol. Struct.*, **985**, 173 (2011).
[19] T. Rosu, M. Negoiu, S. Pasculescu, E. Pahontu, D. Poirier, A. Gulea. *Eur. J. Med. Chem.*, **45**, 774 (2010).
[20] B.D. Wang, Z.Y. Yang, P. Crewdson, D.Q. Wang. *J. Inorg. Biochem.*, **101**, 1492 (2007).
[21] H.G. Li, Z.Y. Yang, B.D. Wang, J.C. Wu. *J. Organomet. Chem.*, **695**, 415 (2010).
[22] Y. Li, Z.Y. Yang, M.F. Wang. *Eur. J. Med. Chem.*, **44**, 4585 (2009).
[23] Y. Ihara, M. Chuda, S. Kuroda, T. Hayabara. *J. Neurol. Sci.*, **170**, 90 (1999).
[24] Y.Z. Cai, Q. Luo, M. Sun, H. Corke. *Life Sci.*, **74**, 2157 (2004).
[25] K.E. Heim, A.R. Tagliaferro, D.J. Bobilya. *J. Nutr. Biochem.*, **13**, 572 (2002).
[26] M.F. Wang, Z.Y. Yang, Y. Li, H.G. Li. *J. Coord. Chem.*, **64**, 2974 (2011).
[27] M. Howe-Grant, K.C. Wu, W.R. Bauer, S.J. Lippard. *Biochemistry*, **15**, 4339 (1976).
[28] A.M. Pyle, J.P. Rehmann, R. Meshoyrer, C.V. Kumar, N.J. Turro, J.K. Barton. *J. Am. Chem. Soc.*, **111**, 3051 (1989).
[29] M.R. Eftink, C.A. Ghiron. *Anal. Biochem.*, **114**, 199 (1981).
[30] C.V. Kumar, R.S. Turner, E.H. Asuncion. *J. Photochem. Photobiol. A Chem.*, **74**, 231 (1993).
[31] M. Eriksson, M. Leijon, C. Hiort, B. Norden, A. Graeslund. *Biochemistry*, **33**, 5031 (1994).
[32] Y. Xiong, X.F. He, X.H. Zou, J.Z. Wu, X.M. Chen, L.N. Ji, R.H. Li, J.Y. Zhou, K.B. Yu. *J. Chem. Soc., Dalton Trans.*, 19 (1999).
[33] C.C. Winterbourn. *Biochem. J.*, **198**, 125 (1981).
[34] W.J. Geary. *Coord. Chem. Rev.*, **7**, 81 (1971).
[35] A.J. Blake, W. Clegg, J.M. Cole. *Crystal Structure Analysis: Principles and Practice*, Oxford University Press, Oxford (2009).
[36] K.K. Narang, V.P. Singh. *Transition Met. Chem.*, **18**, 287 (1993).
[37] F. Marchetti, C. Pettinari, R. Pettinari, A. Cingolani, D. Leonesi, A. Lorenzotti. *Polyhedron*, **18**, 3041 (1999).
[38] J.K. Barton, A. Danishefsky, J. Goldberg. *J. Am. Chem. Soc.*, **106**, 2172 (1984).
[39] A.M. Pyle, J.P. Rehmann, R. Meshoyrer, C.V. Kumar, N.J. Turro, J.K. Barton. *J. Am. Chem. Soc.*, **111**, 3051 (1989).
[40] W.D. Wilson, L. Ratmeyer, M. Zhao, L. Strekowski, D. Boykin. *Biochemistry*, **32**, 4098 (1993).
[41] B.D. Wang, Z.Y. Yang. *J. Fluoresc.*, **18**, 547 (2008).
[42] Y. Li, Z.Y. Yang. *J. Coord. Chem.*, **63**, 1960 (2010).
[43] A.K.R. Lytton-Jean, M.S. Han, C.A. Mirkin. *Anal. Chem.*, **79**, 6037 (2007).
[44] F.Y. Wu, Y.L. Xiang, Y.M. Wu, F.Y. Xie. *J. Lumin.*, **129**, 1286 (2009).
[45] Y.T. Sun, H.Q. Zhang, S.Y. Bie, X.F. Zhou, L. Wang, Y.S. Yan. *J. Lumin.*, **131**, 2299 (2011).
[46] C. Yuan, Z. Zhang, T. Song, G. Wu. *Chem. Res. Chin. Univ.*, **25**, 492 (2009).
[47] Y. Li, Z.Y. Yang, M.F. Wang. *J. Fluoresc.*, **20**, 891 (2010).
[48] S. Satyanarayana, J.C. Dabrowiak, J.B. Chaires. *Biochemistry*, **32**, 2573 (1993).
[49] S. Satyanarayana, J.C. Dabrowiak, J.B. Chaires. *Biochemistry*, **31**, 9319 (1992).
[50] P.H. Proctor, E.S. Reynolds. *Physiol. Chem. Phys. Med. NMR*, **16**, 175 (1984).